

Effect of Sr substitution for Ba on microwave dielectric properties of $\text{Sm}_2(\text{Ba}_{1-x}\text{Sr}_x)(\text{Cu}_{0.5}\text{Zn}_{0.5})\text{O}_5$ ceramics

Soichi Kawaguchi, Hirotaka Ogawa, Akinori Kan*, Eri Tanaka

Faculty of Science and Technology, Meijo University, 1-501 Shiogamaguchi, Tempaku-ku, Nagoya 468-8502, Japan

Available online 24 May 2005

Abstract

The influence of Sr substitution for Ba on the microwave dielectric properties and crystal structure of the $\text{Sm}_2(\text{Ba}_{1-x}\text{Sr}_x)(\text{Cu}_{0.5}\text{Zn}_{0.5})\text{O}_5$ ceramics was studied. However, it was found that the limit of the solid solution was approximately $x=0.4$ from the XRPD patterns. In the single phase region, the sintering temperature dependence of the microwave dielectric properties of the solid solutions was investigated. The dielectric constants of the solid solutions were approximately 18 in the sintering temperature range of 1150–1250°C, whereas the Qf values of the solid solutions strongly depended on the composition x . The Qf values of the solid solution decreased with an increase in composition x ; the differences in the Qf values were attributed to the morphological changes in the samples which arose from the Sr substitution for Ba. However, the Qf value of approximately 65,000 GHz was obtained at $x=0$ in the sintering temperatures ranging from 1150 to 1250°C. The temperature coefficient of resonant frequency (τ_f) of the solid solutions varied from negative to positive values, ranging from -6 to 7 ppm/°C with the Sr substitution for Ba; a near zero τ_f value was obtained at $x=0.05$; a small amount of Sr substitution for Ba was substantially effective in improving the τ_f values of the solid solutions.

© 2005 Elsevier Ltd. All rights reserved.

Keywords: Powders-solid state reaction; X-ray method; Electron microscopy; Dielectric properties

1. Introduction

In recent years, microwave dielectric resonators have been used extensively in the area of wireless communication systems. For the dielectric resonator applications, there are three main requirements. First, the quality factor (Qf) should be high. Second, the low dielectric constant (ϵ_r) is required at the range of the high frequency and the low dielectric constant should be low because the size of resonator is inversely proportional to the square root of its dielectric constant. Third, the temperature coefficient of the resonant frequency (τ_f) should be near zero (a few ppm/°C). However, it is difficult to satisfy the three requirements of the microwave dielectric properties in one material. Most studies of the microwave dielectric properties have focused in particular on the complex perovskite materials such as $\text{Ba}(\text{Mg}, \text{Ta})\text{O}_3$, $\text{Ba}(\text{Zn}, \text{Ta})\text{O}_3$ and $\text{Ba}(\text{Zr}, \text{Zn}, \text{Ta})\text{O}_3$ ^{1–3} although the development of a variety

of microwave dielectric materials which possess the appropriate dielectric properties is necessary for the commercial applications such as the resonator and filter. The Y_2BaCuO_5 compound, i.e., green phase, and the solutions are known as an insulator phase in the area of the high-temperature superconductors; Michel and Raveau⁴ and Watanabe et al.⁵ reported the crystal structure and the microwave dielectric properties of the $\text{Y}_2\text{Ba}(\text{Cu}_{1-x}\text{Zn}_x)\text{O}_5$ solid solutions as a new high- Q material. The crystal structure of Y_2BaCuO_5 compound is known to be an orthorhombic phase with a space group of $Pnma$ (no. 62) and is composed of three types of polyhedra which are Y_2O_{11} , BaO_{11} and CuO_5 polyhedra.⁴ The Y_2O_{11} polyhedron consists of the $\text{Y}(1)\text{O}_7$ and $\text{Y}(2)\text{O}_7$ polyhedra, sharing the common edge and face of $\text{Y}(1)\text{O}_7$ and $\text{Y}(2)\text{O}_7$ polyhedra to form the Y_2O_{11} polyhedron. Moreover, the pentagonal site of Ba^{2+} ion has eleven coordinates; the Cu^{2+} ion is located at the bottom of the CuO_5 pyramid.

In the case of $\text{Sm}_2\text{Ba}(\text{Cu}_{0.5}\text{Zn}_{0.5})\text{O}_5$ ceramics⁶ a near zero τ_f value is required for the commercial applications as mentioned above, though the Qf value of approx-

* Corresponding author.

E-mail address: akan@ccmfs.meijo-u.ac.jp (A. Kan).

imately 65,000 GHz and appropriate temperature coefficient of resonant frequency of $-6.7 \text{ ppm}/^\circ\text{C}$ have been obtained. Thus, in order to obtain the near zero τ_f value, the $\text{Sm}_2(\text{Ba}_{1-x}\text{Sr}_x)(\text{Cu}_{0.5}\text{Zn}_{0.5})\text{O}_5$ ceramics were synthesized and then the microwave dielectric properties and the crystal structure of the solid solutions were investigated in this study.

2. Experimental method

Ceramic pellets such as the $\text{Sm}_2(\text{Ba}_{1-x}\text{Sr}_x)(\text{Cu}_{0.5}\text{Zn}_{0.5})\text{O}_5$ ceramics were prepared via the solid-state reaction method, using Sm_2O_3 , BaCO_3 , SrCO_3 , CuO and ZnO powders with high purity (>99.9%). These materials were weighed on the basis of stoichiometric composition of $\text{Sm}_2(\text{Ba}_{1-x}\text{Sr}_x)(\text{Cu}_{0.5}\text{Zn}_{0.5})\text{O}_5$ ceramics in the composition ranging from 0 to 0.8. The powders were mixed with acetone and calcined at a temperature of 850°C for 20 h in air. The calcined powders were crushed and ground with an organic binder (polyvinyl alcohol). The ground powders were pressed into a pellet of 12 mm in diameter and 7 mm thick under a pressure of 100 MPa. Subsequently, the pellets were sintered in the temperature range of $1050\text{--}1250^\circ\text{C}$ for 2 h in air. The sintering temperatures of each composition were determined by using the differential thermal analysis (DTA) and thermogravimetry (TG). The sintered pellets were polished and annealed at a temperature of 850°C for 2 h in air. The phases of the synthesized materials were identified in terms of the X-ray powder diffraction (XRPD), using the $\text{Cu K}\alpha$ radiation filtered through the Ni foil. The crystal structure and lattice parameters of the samples were refined using the Rietveld analysis program, i.e., RIETAN,⁷ and the atomic distances of the polyhedra were determined. The dielectric constant and Qf values at TE_{011} mode were evaluated by using the Hakki and Coleman method;⁸ the temperature coefficient of resonant frequency was determined from the resonant frequencies at the two temperatures of 20 and 80°C . The microstructure of the samples was investigated by using the field emission scanning electron microscopy (FE-SEM) and energy dispersive X-ray analysis (EDX).

3. Results and discussion

The XRPD patterns of the $\text{Sm}_2(\text{Ba}_{1-x}\text{Sr}_x)(\text{Cu}_{0.5}\text{Zn}_{0.5})\text{O}_5$ ceramics sintered at 1100°C for 2 h in air are shown in Fig. 1; in the composition range of 0–0.4, the single phase which corresponded to the orthorhombic phase was obtained, whereas the formation of four phases, i.e., Sm_2O_3 , $\text{Sr}_{0.75}\text{CuO}_2$, ZnO and unknown phase, was recognized in these profiles of the composition x higher than $x=0.4$. Moreover, the Sr substitution for Ba takes place the peak shifts toward the higher 2θ values with increasing the composition x ; such the peak shifts of the profiles at the composition range of $0 \leq x \leq$

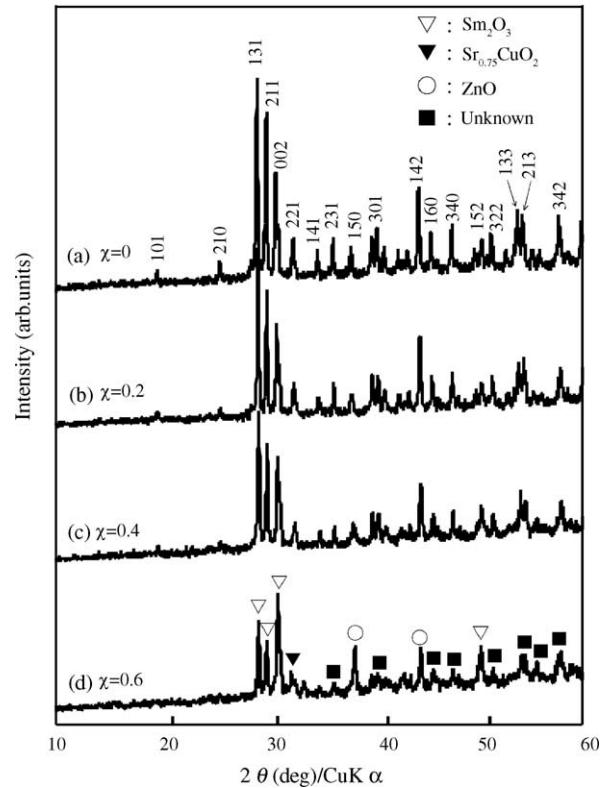


Fig. 1. XRPD pattern of $\text{Sm}_2(\text{Ba}_{1-x}\text{Sr}_x)(\text{Cu}_{0.5}\text{Zn}_{0.5})\text{O}_5$ ($x=0\text{--}0.6$) ceramics at 1100°C for 2 h.

0.4 are due to the differences in the ionic radii of the Sr^{2+} and Ba^{2+} ions. The results of XRPD analysis suggest that the limit of the solid solution is approximately $x=0.4$; the Sr substitution for Ba leads to the decrease in the lattice parameters of the solid solutions. Thus, in order to clarify the effect of Sr substitution for Ba on the crystal structure of $\text{Sm}_2(\text{Ba}_{1-x}\text{Sr}_x)(\text{Cu}_{0.5}\text{Zn}_{0.5})\text{O}_5$ ceramics, the lattice parameters and unit cell volumes of the ceramics were refined in terms of the Rietveld analysis; the results obtained in this study are shown in Fig. 2 as a function of composition x . As for the reliability factors of the Rietveld analysis performed in this study, the reliability factor of weighted pattern (R_{wp}), the reliability factor of pattern (R_p) and the goodness of fit indicator (S) ranged of 3.38–4.07%, 2.66–3.05% and 1.27–1.60, respectively; thus, the refined crystal structure parameters were obtained.

The lattice parameters, a and b , in the single phase region ($0 \leq x \leq 0.4$) linearly decreased, depending on the composition x , whereas the variation in lattice parameter, c , was independent of the composition x as shown in Fig. 2. Thus, it was found that the Sr substitution for Ba exerted an influence on the decreases in the lattice parameters, a and b . The lattice parameters of $\text{Sm}_2(\text{Ba}_{1-x}\text{Sr}_x)(\text{Cu}_{0.5}\text{Zn}_{0.5})\text{O}_5$ ($x=0.5$) ceramic, however, exhibited the similar values to those at $x=0.4$. Such variations in the lattice parameters imply that the indicate of solid solutions is approximately $x=0.4$. Although the influences of Sr substitution for Ba on the lattice

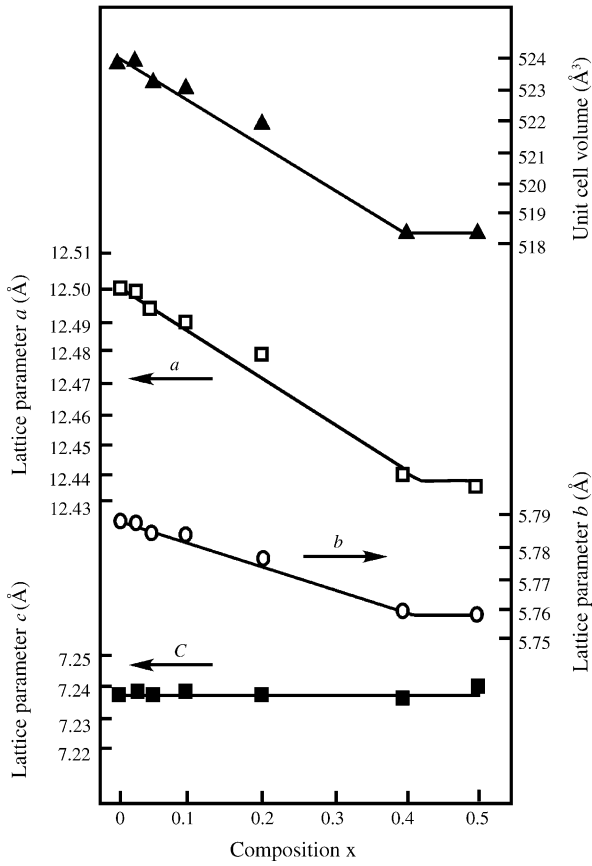


Fig. 2. Effect of Sr substitution for Ba on lattice parameters and unit cell volume of $\text{Sm}_2(\text{Ba}_{1-x}\text{Sr}_x)(\text{Cu}_{0.5}\text{Zn}_{0.5})\text{O}_5$ ceramics sintered at 1100 °C for 2 h in air.

parameters and unit cell volume were clarified, the interrelationships between the variations in the atomic distances of polyhedra and the Sr substitution for Ba have not been evaluated. Thus, the atomic distances of polyhedra were determined on the basis of refined crystal parameters. In the green phase-type crystal structure, the crystal structure is composed of three-types polyhedra, i.e., Sm_2O_{11} , AO_{11} (A = Ba and Sr) and MO_5 (M = Cu and Zn), respectively. The remarkable variations in the atomic distances of AO_{11} were observed in

Table 1
Atomic distances of AO_{11} (A = Ba and/or Sr) polyhedron

Atomic distances (Å)	x = 0	x = 0.4
A-O1	3.08	2.34
A-O2	2.98	2.96
A-O3	2.89	2.88
A-O'1	3.26	3.83
A-O'2	3.11	3.15
A-O'3	2.52	2.61
O1-O1	2.70	1.30
O2-O2	2.97	2.98
O'1-O'1	3.08	4.46
O'2-O'2	2.82	2.78

comparison with those of the Sm_2O_{11} and MO_5 polyhedra; the results are shown in Fig. 3 and Table 1, respectively. The atomic distances, such as O1-O1 and O'2-O'2, in the AO_{11} polyhedra were decreased by the Sr substitution for Ba, resulting in the decrease in the volume of AO_{11} polyhedra. Thus, the decreases in the lattice parameters and unit cell volumes of the solid solutions as mentioned above are related to the variations in the atomic distances in the AO_{11}

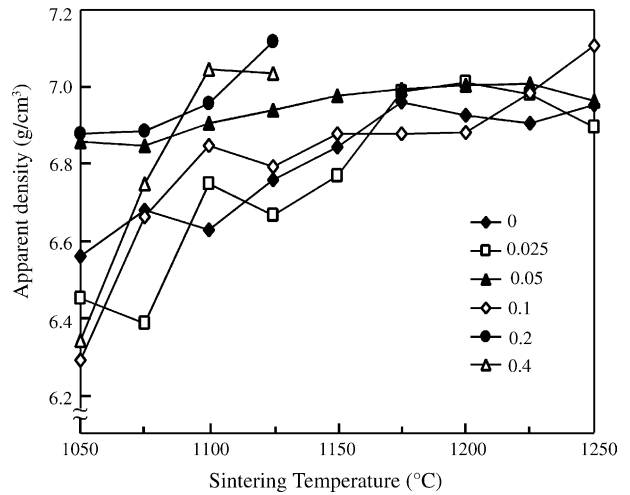


Fig. 4. Relationship between the apparent density and composition of $\text{Sm}_2(\text{Ba}_{1-x}\text{Sr}_x)(\text{Cu}_{0.5}\text{Zn}_{0.5})\text{O}_5$ (x = 0–0.4) ceramics.

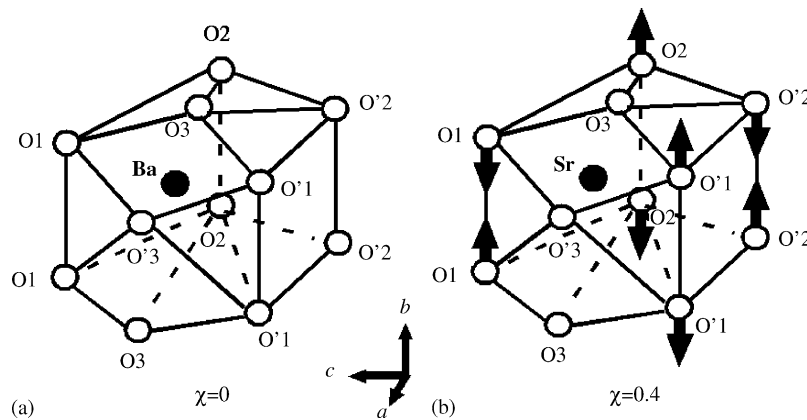


Fig. 3. Variations in atomic distances in AO_{11} polyhedron of $\text{Sm}_2(\text{Ba}_{1-x}\text{Sr}_x)(\text{Cu}_{0.5}\text{Zn}_{0.5})\text{O}_5$ ceramics caused by Sr substitution for Ba.

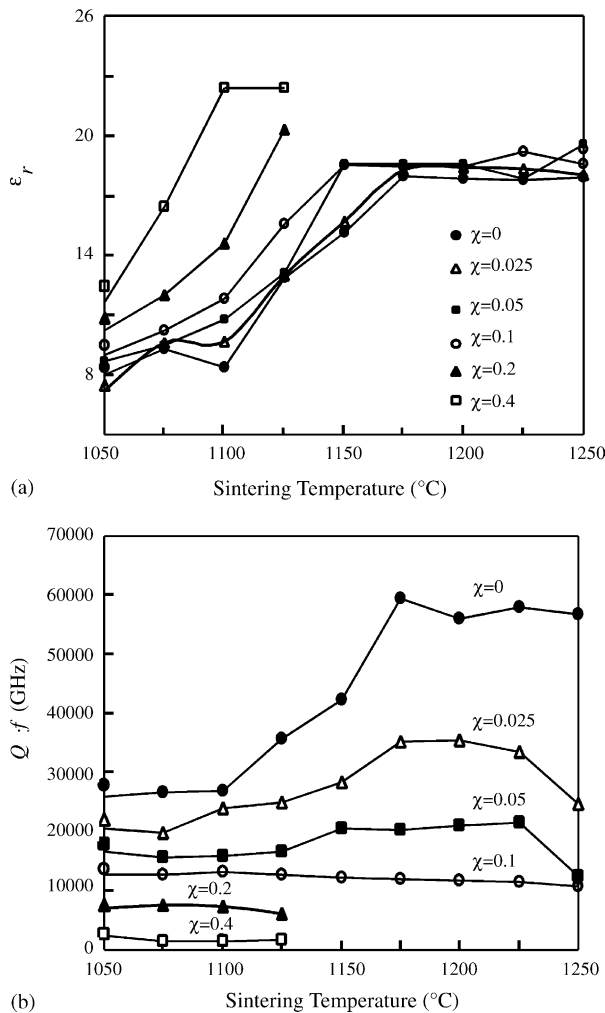


Fig. 5. Sintering temperature dependence of dielectric constant (ϵ_r) and quality factor (Qf) of $\text{Sm}_2(\text{Ba}_{1-x}\text{Sr}_x)(\text{Cu}_{0.5}\text{Zn}_{0.5})\text{O}_5$ ($x=0-0.4$) ceramics.

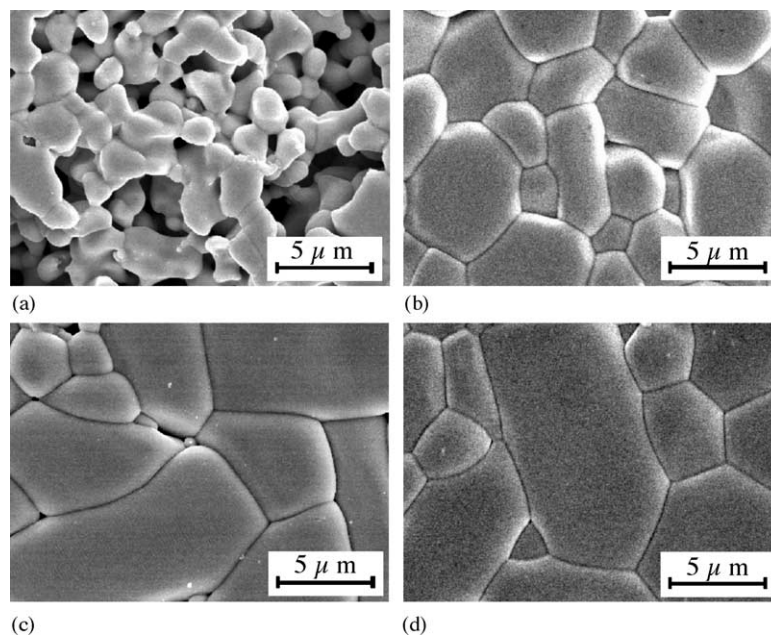


Fig. 6. FE-SEM photographs of $\text{Sm}_2\text{BaCu}_{0.5}\text{Zn}_{0.5}\text{O}_5$ ceramics sintered at (a) 1100 °C, (b) 1150 °C, (c) 1200 °C and (d) 1225 °C for 2 h in air.

polyhedra which depend on the differences in the ionic radii of Ba^{2+} and Sr^{2+} ions.

The effect of sintering temperature on the apparent density of the $\text{Sm}_2(\text{Ba}_{1-x}\text{Sr}_x)(\text{Cu}_{0.5}\text{Zn}_{0.5})\text{O}_5$ solid solutions in the composition range of 0–0.4 is shown in Fig. 4. The apparent density of the sintered sample at $x=0$ was approximately 6.53 g/cm^3 ; and this value corresponds to 88.38% of the theoretical value of the sample obtained at the sintering temperature of 1100 °C. With increasing the composition x from 0 to 0.4, the saturation value of the apparent densities shifted toward the lower sintering temperatures; the Sr substitution for Ba enables the $\text{Sm}_2(\text{Ba}_{1-x}\text{Sr}_x)(\text{Cu}_{0.5}\text{Zn}_{0.5})\text{O}_5$ solid solution to reach its maximum density at a low sintering temperature. The sintering temperature dependence of dielectric constant and the Qf values of $\text{Sm}_2(\text{Ba}_{1-x}\text{Sr}_x)(\text{Cu}_{0.5}\text{Zn}_{0.5})\text{O}_5$ solid solutions ($0 \leq x \leq 0.4$) is shown in Fig. 5(a and b), respectively. The dielectric constants of the samples saturated in the apparent densities were approximately 18; the remarkable differences in the dielectric constants which depended on the composition x were not recognized. Thus, it is considered that the sintering temperature dependence of the dielectric constant of the solid solutions is strongly effected by the variations in the apparent density. The Qf values of the solid solution at $x=0$ increased with increasing the sintering temperatures from 1050 to 1175 °C, and then the saturation value of approximately 60,000 GHz was obtained in the temperature range of 1175–1250 °C. Such an increase in the Qf value of the $x=0$ samples is due to the grain growth of the samples because it is generally known that the grain growth exert an influence on the improvement in Qf value.^{9,10} However, the Qf values of the solid solutions sintered at the same sintering temperature were decreased with increasing the composition x ; in the case of sintering temperature of 1125 °C, the Qf values of the solid solutions decreased from 35,804 to 1617 GHz

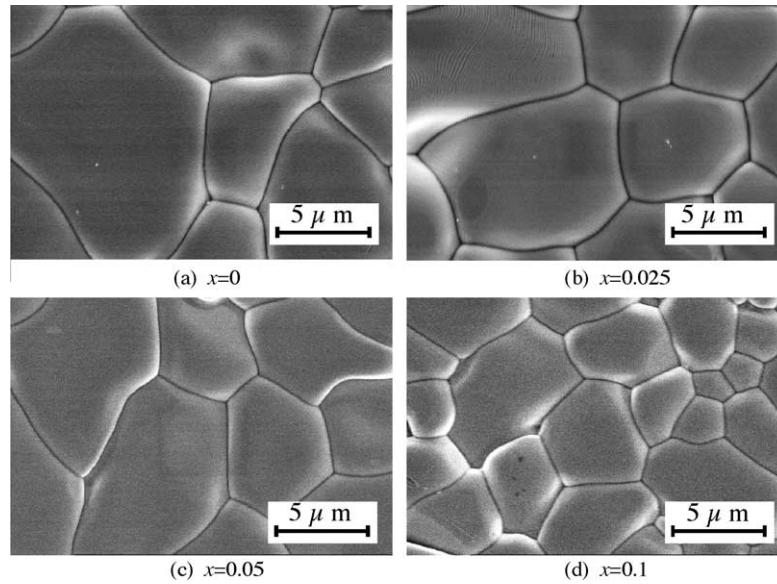


Fig. 7. Microstructures of $\text{Sm}_2(\text{Ba}_{0.95}\text{Sr}_{0.05})(\text{Cu}_{0.5}\text{Zn}_{0.5})\text{O}_5$ ceramics ($x=0-0.4$) sintered at 1225°C for 2 h in air.

in the composition range of 0–0.4. Such a variation in the Qf values of the solid solutions may relate with the morphological changes in the samples. Thus, the microstructures of the samples were investigated by using the FE-SEM. Fig. 6

shows the microstructure of the samples ($x=0-0.4$) sintered at 1225°C for 10 h in air. The morphological changes in the samples with $x=0$ caused by the differences in the sintering temperature were investigated by using FE-SEM; the results were shown in Fig. 6. The change in the grain size of the solid solution can be seen in the FE-SEM micrographs when increasing the sintering temperature. Thus, it is considered that the improvement in Qf which depend on the sintering time is attributed to the grain growth of the samples. As for the microstructure of the samples with different compositions, with increasing the composition x from 0 to 0.4 the decrease in the grain size of the samples was observed as shown in Fig. 7; this result may be due to the instability of phase. Thus, the decrease in the Qf value of the samples which depends on com-

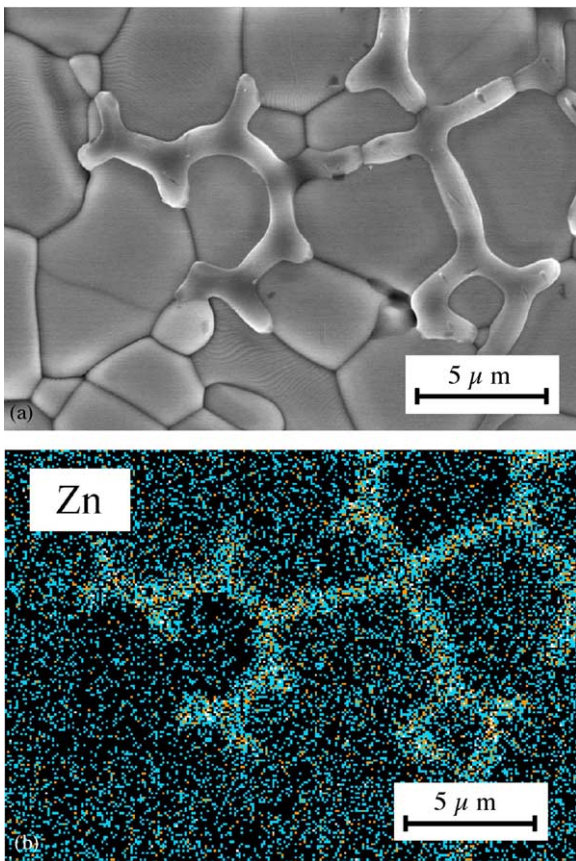


Fig. 8. FE-SEM photographs and EDX result of $\text{Sm}_2(\text{Ba}_{0.95}\text{Sr}_{0.05})(\text{Cu}_{0.5}\text{Zn}_{0.5})\text{O}_5$ ceramics sintered at 1250°C for 2 h in air.

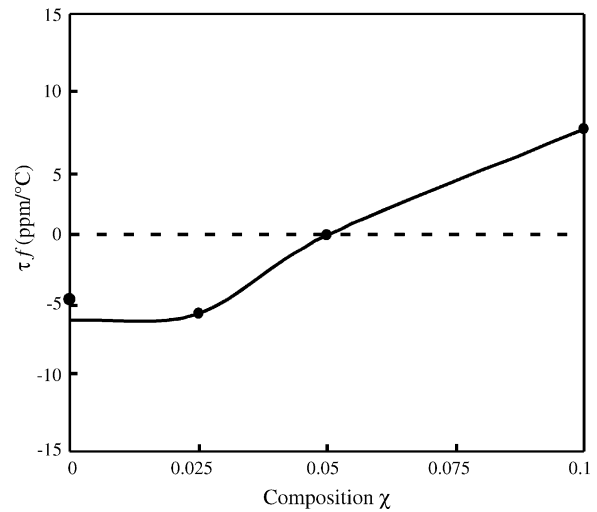


Fig. 9. Effect of Sr substitution for Ba on temperature coefficient of resonant frequency of $\text{Sm}_2(\text{Ba}_{1-x}\text{Sr}_x)(\text{Cu}_{0.5}\text{Zn}_{0.5})\text{O}_5$ ceramics sintered at 1200°C for 2 h in air.

position x may relate to the morphological changes in the samples. At the sintering temperatures $>1175^\circ\text{C}$ for $x=0$, 0.025 and 0.05 samples, the Qf values of samples at $x=0$ were approximately constant, whereas those of the samples at $x=0.025$ and 0.05 decreased at the sintering temperature of 1250°C in comparison with those sintered in the temperature range of 1175 – 1225°C . This result was examined in terms of FE-SEM and EDX analysis; the microstructure of the samples ($x=0.05$) sintered at 1250°C were investigated in order to clarify the relationship between the microstructure and Qf values. The EDX results of the $x=0$ sample showed that the grain of the elements of sample had a stoichiometric composition of $\text{Sm}_2\text{Ba}(\text{Cu}_{0.5}\text{Zn}_{0.5})\text{O}_5$ compound. On the other hand, the microstructure of the sample ($x=0.05$) showed the presence of a secondary phase at the grain boundary as shown in Fig. 8(a); from EDX analysis, the secondary phase was found to be a zinc rich phase (Fig. 8(b)). Thus, the decrease in the Qf value of sample ($x=0.05$) sintered at 1250°C is due to the secondary phase which arises from the decomposition of the $\text{Sm}_2(\text{Ba}_{0.95}\text{Sr}_{0.05})(\text{Cu}_{0.5}\text{Zn}_{0.5})\text{O}_5$ compound. The variations in τ_f values of $\text{Sm}_2(\text{Ba}_{1-x}\text{Sr}_x)(\text{Cu}_{0.5}\text{Zn}_{0.5})\text{O}_5$ solid solutions in the composition range of 0–0.1 were shown in Fig. 9; the τ_f values varied from -5 to $6\text{ ppm}/^\circ\text{C}$. As a result, a near zero τ_f value was obtained at $x=0.05$, and it was clarified that the Sr substitution for Ba is effective in improving the τ_f values of the solid solutions.

4. Conclusions

The microwave dielectric properties, crystal structure and microstructure of $\text{Sm}_2(\text{Ba}_{1-x}\text{Sr}_x)(\text{Cu}_{0.5}\text{Zn}_{0.5})\text{O}_5$ ($x=0$ – 0.8) ceramics were investigated; the XRPD patterns of the ceramics showed a single phase in the composition range of 0–0.4, resulting in the peak shifts toward the higher angles of 2θ values. The lattice parameters of the $\text{Sm}_2(\text{Ba}_{1-x}\text{Sr}_x)(\text{Cu}_{0.5}\text{Zn}_{0.5})\text{O}_5$ ceramics linearly decreased with increasing the composition x from 0 to 0.4; these values were almost constant at $x=0.5$. Therefore, the limit of the solid solutions was found to be approximately $x=0.4$, and then the decreases in the lattice parameters are attributed to the difference in the ionic radii of Ba^{2+} and Sr^{2+} ions.

Moreover, the crystal structure analysis in terms of the Rietveld analysis revealed that the atomic distances in the AO_{11} ($A = \text{Ba}, \text{Sr}$) polyhedra were decreased by the Sr substitution for Ba; such decreases in the atomic distances in the polyhedra led to the decrease in the lattice parameters. As for the microwave dielectric properties, the significant variations in the dielectric constant which depended on the composition x were not recognized in the sintering temperature range of 1175 – 1250°C ; these values were approximately 18. The Qf values of the solid solutions extremely decreased from 60,000 to 10,000 GHz with increasing the composition x ; this result was due to the morphological change in the samples caused by the Sr substitution for Ba. The τ_f values varied from -6 to $7\text{ ppm}/^\circ\text{C}$, depending on the composition x and then a near zero τ_f value was obtained at $x=0.05$.

References

- Nomura, S., Toyama, K. and Kaneta, K., $\text{Ba}(\text{Mg}_{1/3}\text{Ta}_{2/3})\text{O}_3$ ceramics with temperature-stable high dielectric constant and low microwave loss. *Jpn. J. Appl. Phys.*, 1982, **21**, 624–626.
- Wakino, K., Murata, M. and Tamura, H., Far infrared reflection spectra of $\text{Ba}(\text{Zn},\text{Ta})\text{O}_3$ – BaZrO_3 dielectric resonator material. *J. Am. Ceram. Soc.*, 1986, **69**, 34–38.
- Venkatesh, J., Sivasubramanian, V., Subramanian, V. and Murthy, V. R. K., Far-IR reflectance study on B-site disordered $\text{Ba}(\text{Zn}_{1/3}\text{Ta}_{2/3})\text{O}_3$ dielectric resonator. *Mater. Res Bull.*, 2000, **35**, 1325–1332.
- Michel, C. and Raveau, B., A_2BaCuO_5 ($A = \text{Y}, \text{Sm}, \text{Eu}, \text{Gd}, \text{Dy}, \text{Ho}, \text{Er}, \text{Yb}$) oxides. *J. Solid Chem.*, 1982, **43**, 73–80.
- Watanabe, M., Ogawa, H., Ohsato, H. and Humphreys, C., Microwave dielectric of $\text{Y}_2\text{Ba}(\text{Cu}_{1-x}\text{Zn}_x)\text{O}_5$ solid solutions. *Jpn. J. Appl. Phys.*, 1998, **37**, 5360–5363.
- Kan, A., Ogawa, H., Watanabe, M., Hatanaka, S. and Ohsato, H., Microwave dielectric properties of $\text{Sm}_2\text{Ba}(\text{Cu}_{1-x}\text{Zn}_x)\text{O}_5$ solid solutions. *Jpn. J. Appl. Phys.*, 1999, **38**, 5629–5632.
- Izumi, F., *Rietveld Method*, ed. R. A. Young, Oxford University Press, Oxford, 1993, Chapter 13.
- Hakki, B. W. and Coleman, P. D., A dielectric resonator method of measuring inductive capacities in the millimeter range. *IRE Trans. Microwave Theory Tech.*, 1960, 402–410, MTT-8.
- Matsumoto, H., Tamura, H. and Wakino, K., $\text{Ba}(\text{Mg},\text{Ta})\text{O}_3$ – BaSnO_3 high- Q dielectric resonator. *Jpn. J. Appl. Phys.*, 1991, **30**, 2347–2349.
- Tzou, W. C., Yang, C. F., Chen, Y. C. and Cheng, P. S., Improvements in the sintering and microwave properties of BiNbO_4 Microwave ceramics by V_2O_5 addition. *J. Eur. Ceram. Soc.*, 2000, **20**, 991–996.